

# NJC

Accepted Manuscript



This is an *Accepted Manuscript*, which has been through the Royal Society of Chemistry peer review process and has been accepted for publication.

*Accepted Manuscripts* are published online shortly after acceptance, before technical editing, formatting and proof reading. Using this free service, authors can make their results available to the community, in citable form, before we publish the edited article. We will replace this *Accepted Manuscript* with the edited and formatted *Advance Article* as soon as it is available.

You can find more information about *Accepted Manuscripts* in the [Information for Authors](#).

Please note that technical editing may introduce minor changes to the text and/or graphics, which may alter content. The journal's standard [Terms & Conditions](#) and the [Ethical guidelines](#) still apply. In no event shall the Royal Society of Chemistry be held responsible for any errors or omissions in this *Accepted Manuscript* or any consequences arising from the use of any information it contains.



[www.rsc.org/njc](http://www.rsc.org/njc)



Journal Name

ARTICLE

## Surfactant-free Pd@pSiO<sub>2</sub> yolk-shell nanocatalyst for selective oxidation of primary alcohols to aldehydes

Aram Kim,<sup>a†</sup> Hee Seon Bae,<sup>a†</sup> Ji Chan Park,<sup>\*b</sup> Hyunjoon Song<sup>c</sup> and Kang Hyun Park<sup>\*a</sup>

Received 00th January 20xx,  
Accepted 00th January 20xx

DOI: 10.1039/x0xx00000x

www.rsc.org/

Combined high catalytic activity and thermal stability were achieved with a well-structured, surfactant-free Pd@porous SiO<sub>2</sub> yolk-shell nanostructure, resulting from the entirely exposed Pd core particles and highly porous silica shells. Pd@SiO<sub>2</sub> core-shell nanoparticles were synthesized by a water-in-oil microemulsion method for direct silica coating of as-prepared tiny Pd nanoparticles. Hydrothermal etching and subsequent high thermal treatment generated large pores in the silica shells and facilitated complete removal of surfactants around the core particles. The surfactant-free Pd@pSiO<sub>2</sub> yolk-shell nanoparticles efficiently catalyzed the oxidation of benzyl alcohol as well as that of various substituted benzyl alcohols.

### Introduction

High activity, stability, selectivity, recovery, and reusability are some specific and nonnegotiable prerequisites in the field of catalysis. Homogeneous catalyst systems are generally considered to have high activity and specific selectivity, whereas heterogeneous catalysts offer the advantages of facile separation of the catalyst system from the products with improved stability and reusability of the catalyst. Recently, several researches have focused on developing new catalysts that combine the positive aspects of both catalyst systems. Owing to such efforts, many nanomaterial catalyst systems have been developed that possess notably high catalytic activity resulting from their high surface-to-volume ratio, notable chemical and thermal stability, durability, facile recovery, and reusability<sup>1-5</sup>.

Various approaches and methods have been proposed for developing multicomponent hybrid nanomaterials with diverse chemical compositions and morphologies that not only have the original properties of the components but also have new properties derived from the incorporation of each component<sup>6-14</sup>. Furthermore, the catalytic performance of hybrid nanomaterials has been found to be remarkably superior to that of single-component nanomaterials in diverse reactions. For instance, it was observed that hybrid Au-graphene oxide (GO) nanosheets, dumbbell- and flower-like Au-Fe<sub>3</sub>O<sub>4</sub> heterostructures, and trimetallic Au@PdPt core-

shell nanoparticles exhibited excellent catalytic activity in the reduction of nitro compounds<sup>15-17</sup>. Furthermore, Pd nanoparticles supported on GO, Pd-Fe<sub>3</sub>O<sub>4</sub>@carbon hybrid nanoparticles, and Pd-Fe<sub>3</sub>O<sub>4</sub> nanoparticles showed high catalytic activity and stability in the Suzuki-Miyaura coupling reaction<sup>18-20</sup>.

In a recent work in our laboratory, hybrid nanoparticles with various structures and chemical compositions were successfully developed and utilized as catalysts for organic reactions such as azide-alkyne cycloaddition reactions, reduction of nitroarenes, and propargylation reactions. Our efforts have focused on developing Pd hybrid nanoparticles with bifunctional structures that contain active Pd nanoparticles embedded on metal oxide supports or carbon-based materials and on verifying the influence of porosity and organic capping agents on the effective catalytic activity of these nanoparticles in the Suzuki coupling reaction<sup>21-26</sup>.

The oxidation of alcohols to carbonyl compounds is a fundamentally important organic transformation, and thus, extensive effort has been devoted to verifying the catalytic activity and, in particular, to achieving a selectivity of heterogeneous catalysts in the oxidation of alcohols<sup>27-33</sup>. Recently, Au, Pd, Mn<sub>2</sub>O<sub>3</sub>, Fe<sub>3</sub>O<sub>4</sub>, TiO<sub>2</sub>-based hybrid nanoparticles were found to show high efficiency as a catalyst for the oxidation of alcohols<sup>34-40</sup>.

Herein, we report the synthesis of surfactant-free Pd@pSiO<sub>2</sub> yolk-shell nanoparticles and their high catalytic activity resulting from entirely exposed Pd core particles and highly porous silica shells. These hybrid Pd@pSiO<sub>2</sub> yolk-shell nanoparticles efficiently catalyze the oxidation of benzyl alcohol as well as that of various substituted benzyl alcohols.

### Experimental

#### General remarks

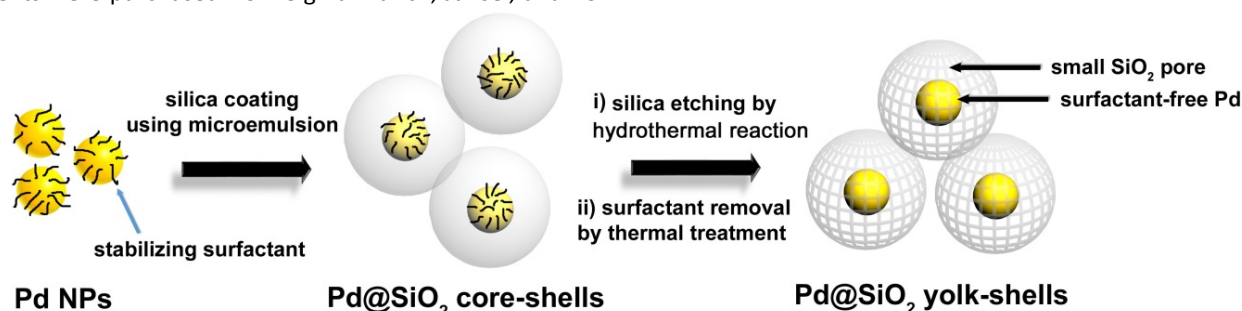
<sup>a</sup> Department of Chemistry and Chemistry Institute for Functional Materials, Pusan National University, Busan 609-735, Korea. Tel:+82-51-510-2238 Fax:+82-51-980-5200 \*E-mail: chemistry@pusan.ac.kr

<sup>b</sup> Clean Fuel Laboratory, Korea Institute of Energy Research, Daejeon, 305-343, Korea.

<sup>c</sup> Department of Chemistry, Korea Advanced Institute of Science and Technology, Daejeon 305-701, Korea

† These authors contributed equally to this work.

Reagents were purchased from Sigma Aldrich, Junsei, and TCI.



Scheme 1. Synthetic scheme of Pd@pSiO<sub>2</sub> yolk-shell nanoparticles.

The chemicals were used as received without further purification. The prepared hybrid nanoparticles were characterized by using TEM and HRTEM (Philips F20 Tecnai, operated at 200 kV, KAIST), XRD (Rigaku D/MAX-RB, 12 kW), ICP-AES (POLY SCAN 60 E), BELSORP-HP (BEL Japan Inc.), and BELSORP mini-II (BEL Japan Inc.) instruments.

The catalytic reaction products were analyzed by <sup>1</sup>H-NMR spectroscopy, where the spectra were acquired on a Varian Mercury Plus (300 MHz) instrument.

#### Synthesis of hybrid surfactant-free Pd@pSiO<sub>2</sub> yolk-shell nanoparticles

Synthesis of hybrid surfactant-free Pd@pSiO<sub>2</sub> yolk-shell nanoparticles has been described in detail in our previous publication<sup>21</sup>. The experimental procedure was conducted in three steps, synthesis of: (1) Pd nanoparticles, (2) Pd@SiO<sub>2</sub> core-shell nanoparticles, and (3) surfactant-free Pd@pSiO<sub>2</sub> yolk-shell nanoparticles.

In the first step, uniform Pd nanoparticles were obtained by slowly heating the Pd-surfactant complexes using Pd(acac)<sub>2</sub>, trioctylphosphine (TOP), and oleylamine to 503 K. In order to acquire Pd@SiO<sub>2</sub> core-shell nanoparticles, the Pd particle dispersion in cyclohexane was then added to a mixture of Igepal CO-630 and aqueous ammonia solution in cyclohexane under stirring. tetramethyl orthosilicate (TMOS) and octadecyltrimethoxysilane (C<sub>18</sub>TMS) were added to the aforementioned reaction mixture under stirring at room temperature. The desired Pd@pSiO<sub>2</sub> yolk-shell nanoparticles were obtained by heating the aqueous dispersion of Pd@SiO<sub>2</sub> core-shell nanoparticles in an oven at 383 K for 12 h. After centrifugation, washing, and drying, the formed powders were slowly heated and aged from room temperature to 773 K at a rate of 4 K/min under a continuous hydrogen flow.

#### General procedure for the oxidation of benzyl alcohols

Under the optimal reaction conditions, the calcined Pd@pSiO<sub>2</sub> yolk-shell nanoparticles (7.1 mg, 0.1 mol% with respect to the substrate), benzyl alcohol (0.1 mL, 1 mmol), sodium periodate (1.07 g, 5 mmol), and 1,4-dioxane (5.0 mL) were introduced into a 25 mL stainless steel reactor. The mixture was stirred at 150 °C for 12 h. After cooling to room temperature, the Pd@pSiO<sub>2</sub> yolk-shell nanoparticles were separated from the mixture by simple filtration, and the reaction product was extracted into dichloromethane and washed with sodium bicarbonate solution to eliminate the salts. The organic layer

was dried over anhydrous magnesium sulfate and concentrated under reduced pressure.

## Results and discussion,

### Catalyst characterization

Spherical Pd nanoparticles with a diameter of 3.4±0.2 nm were formed by thermal decomposition of the Pd-surfactant complexes<sup>21, 41</sup>. The phosphine-stabilized Pd nanoparticles, which possessed inherent catalytic activity, were successfully coated with uniform layers of silica using a well-known water-in-oil microemulsion method<sup>42</sup>.

The structure of the Pd@SiO<sub>2</sub> core-shell nanoparticles consisting of a Pd core and silica shell obviously contributed to securing the durability and sustainability of the assembly and preventing agglomeration of individual Pd nanoparticles. In terms of structure, the surface of Pd, which possesses catalytically active sites, was completely blocked by the silica shell; thus, it was necessary to adequately dissolve the silica components adjacent to the Pd core.

In order to prevent an agglomeration of Pd core, Pd nanoparticles were coated with silica shell with a thickness of 9.74±1.5 nm. The surface of Pd in Pd@SiO<sub>2</sub> core-shells was completely blocked by the dense silica before the hydrothermal reaction (Figure 1a). Under hydrothermal conditions, it was possible to preferentially and randomly generate multiple large pores inside the silica shell, which practically turned the core-shell structure into the yolk-shell structure (Figure 1b). C<sub>18</sub>TMS as long chain alkyl siloxanes engenders irregular pores as it calcined at high temperature.

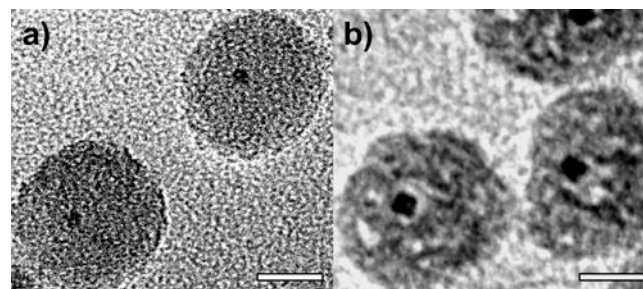
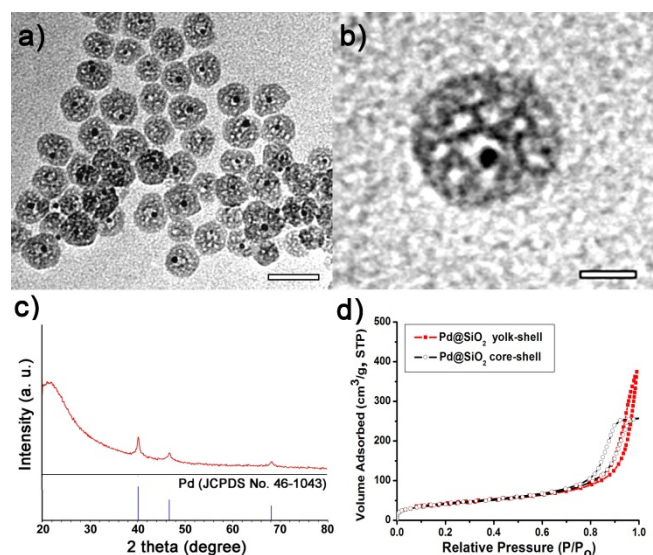


Fig. 1 TEM images of (a) Pd@SiO<sub>2</sub> core-shell and (b) Pd@pSiO<sub>2</sub> yolk-shell nanoparticles before thermal treatment. All bars represent 10 nm.

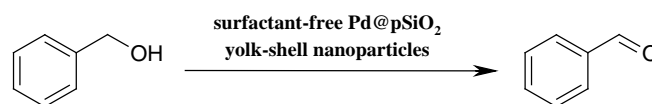


**Fig. 2** (a) TEM, (b) HRTEM images and (c) XRD pattern of the surfactant-free Pd@pSiO<sub>2</sub> yolk-shell nanoparticles, and (d) N<sub>2</sub> adsorption-desorption isotherms of the Pd@SiO<sub>2</sub> core-shell (○) and Pd@pSiO<sub>2</sub> yolk-shell (■). The bars represent 40 nm (a) and 10 nm (b), respectively.

Subsequently, through thermal treatment, all organic residues such as C<sub>18</sub>TMS and TOP surfactants could be pyrolyzed to transform the silica shell into a more porous and less dense form, thereby entirely exposing the surface of the active Pd core nanoparticle and improving the diffusion rate of the reactant through the porous silica shell. As a result, irregular pores could be formed inside the silica shells, and surfactant-free Pd@pSiO<sub>2</sub> yolk-shell nanoparticles were generated.

In the TEM images of Pd@pSiO<sub>2</sub> yolk-shells, all Pd nanoparticles are located in hollow-typed silica shells having many pores. In this case, the active Pd surface could be well exposed to reactants (Figure 2a-b). The size of the Pd core particle after thermal treatment was determined to be 3.5±0.3 nm from the TEM image. This value is nearly identical to the value of 3.4 nm obtained for the particle without thermal treatment, which demonstrates the high stability of the Pd particles inside the silica shells. The HRTEM image clearly shows bright regions that indicate the generation of large pores and vacant sites around a single Pd core and inside a single silica shell (Figure 2b). The X-ray diffraction (XRD) pattern of the surfactant-free Pd@pSiO<sub>2</sub> yolk-shell nanoparticles was indexed to the face-centered cubic (fcc) Pd structure (Figure 2c, JCPDS No. 46-1043). N<sub>2</sub> sorption analysis at 77 K produced type IV adsorption-desorption with type H3 hysteresis, and the BET (Brunauer-Emmett-Teller) surface area was calculated to be 145 m<sup>2</sup> g<sup>-1</sup> (Figure 2d). And the small silica pore size of Pd@pSiO<sub>2</sub> yolk-shells was determined to be about 1.9 nm from the desorption branch. The total pore volume of the Pd@SiO<sub>2</sub> core-shell nanoparticles was 0.40 cm<sup>3</sup> g<sup>-1</sup>, whereas the pore volume of the surfactant-free Pd@pSiO<sub>2</sub> yolk-shell nanoparticles was 40% higher with a value of 0.57 cm<sup>3</sup> g<sup>-1</sup>. These data prove that significantly more pores are retained in the yolk-shell structure than in the core-shell due to the partial silica etching step. The Pd loading in the

Pd@pSiO<sub>2</sub> yolk-shell nanoparticles was determined to be 1.5 wt%.



**Scheme 2.** Oxidation reaction of benzyl alcohol to benzaldehyde catalyzed by surfactant-free Pd@pSiO<sub>2</sub> yolk-shell nanoparticles.

**Table 1** Oxidation reaction of benzyl alcohol using surfactant-free Pd@pSiO<sub>2</sub> catalyst<sup>a</sup>.

Entry	Temp (°C)	Time (h)	O <sub>2</sub> source	Solvent	Conv. (%) <sup>b</sup>
1	150	12	Air	Toluene	0
2	100	6	Air	DMF	1
3	100	1	Air	1,4-dioxane	23
4	100	6	Air	1,4-dioxane	32
5	150	6	Air	1,4-dioxane	40
6	150	12	Air	1,4-dioxane	51
7	150	12	NaIO <sub>4</sub>	1,4-dioxane	>99
8	150	12	<i>tert</i> -BuOOH	1,4-dioxane	40
9	150	12	H <sub>2</sub> O <sub>2</sub>	1,4-dioxane	6
10	150	12	NaOCl	1,4-dioxane	2

<sup>a</sup> Reaction condition: benzyl alcohol (1 mmol), Pd@pSiO<sub>2</sub> (0.1 mol% with respect to benzyl alcohol), oxidant (5 equiv. to the substrate) or air (5 atm).

<sup>b</sup> Determined by <sup>1</sup>H-NMR. Conversion is based on the amount of benzyl alcohol used.

### Reaction test

The hybrid, surfactant-free Pd@pSiO<sub>2</sub> yolk-shell nanoparticles were employed as catalysts for the alcohol oxidation reaction (Scheme 2). The optimal reaction conditions for the oxidation of benzyl alcohol were determined by varying the reaction temperature, time, oxygen sources, and solvents in the presence of the hybrid Pd catalyst (Table 1). This oxidation reaction resulted in the formation of benzaldehyde as the desired product. 1,4-Dioxane was found to be the most suitable solvent for the reaction (entries 1-3, Table 1). On the other hand, dimethylformamide and toluene were found to be inappropriate (entries 1-2, Table 1).

The oxidation of benzyl alcohol was also affected to some degree by the reaction time and temperature. With prolonged reaction time, the conversion of benzyl alcohol to benzaldehyde increased (entries 3-4, Table 1). More product was obtained at high temperature (150 °C), which was achieved by using a stainless steel reactor (entries 4-5, Table 1). Accordingly, a reaction time of 12 h and reaction temperature of 150 °C were chosen for the optimization studies (entry 6, Table 1). Various oxygen sources such as NaIO<sub>4</sub>, *tert*-BuOOH, H<sub>2</sub>O<sub>2</sub>, and NaOCl were used instead of air to find a more effective oxygen source (entries 7-10, Table 1). The conversion increased drastically upon replacement of air as an oxidant with NaIO<sub>4</sub>. However, the other oxidants such as

*tert*-BuOOH, H<sub>2</sub>O<sub>2</sub>, and NaOCl were not more effective than air. The type of oxygen source used is thus regarded as an important factor influencing the reaction efficiency. The optimal reaction conditions for alcohol oxidation catalyzed by 0.1 mol% of surfactant-free Pd@pSiO<sub>2</sub> yolk-shell nanoparticles were determined to be as follows: oxygen source: NaIO<sub>4</sub>, solvent: 1,4-dioxane, temperature: 150 °C, duration: 18 h (entry 7, Table 1).

The catalytic activity of Pd@pSiO<sub>2</sub> yolk-shell nanocatalyst was also compared with that from previous reported catalysts such as Fe<sub>3</sub>O<sub>4</sub>@MIL-101, Au/TiO<sub>2</sub>, Fe<sup>3+</sup>/TiO<sub>2</sub>, Au/NiAl-LDH, Cu<sub>2</sub>O/Au and Mn<sub>2</sub>O<sub>3</sub> nanorod (Table 2).

The oxidation of various substituted benzyl alcohols was found to be efficiently catalyzed by the surfactant-free Pd@pSiO<sub>2</sub> yolk-shell nanoparticles under the optimal conditions (Table 3). In general, the results showed that benzyl alcohols substituted with electron donating groups furnished higher yields than those substituted with electron-withdrawing groups. Benzyl alcohols bearing methoxy, methyl, and nitro substituents afforded the corresponding benzaldehyde with more than 90% conversion yield (entries 1–4, Table 3). On the other hand, halogen-substituted benzyl alcohols were not adequately oxidized (entries 5–9, Table 3). The relative reactivity of halogen substituents ranked in the following order: Br<sup>-</sup> > Cl<sup>-</sup> > F<sup>-</sup> (entries 5–7, Table 3). Notably, the substituted positions on the phenyl ring (such as ortho-, meta-, and para-) were not found to have a critical effect on the conversion yield (entries 7–9, Table 3). Furthermore, this catalyst was found to be useful for the oxidation of secondary aryl alcohols such as 1-phenylethanol, as well as primary aryl alcohols (entry 10, Table 3).

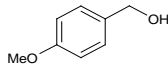
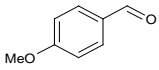
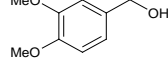
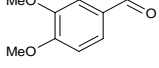
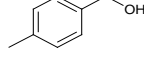
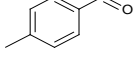
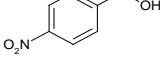
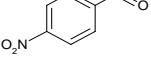
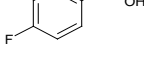
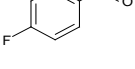
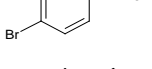
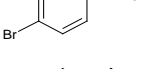
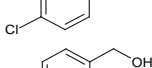
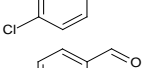
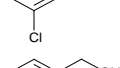
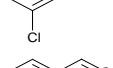
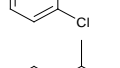
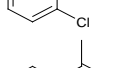
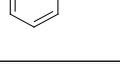
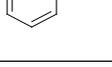
After the reaction, Pd@pSiO<sub>2</sub> yolk-shell nanoparticles were readily separated by centrifugation and could be reused three more times under the same reaction condition (Figure 3). The structure of yolk-shell nanoparticle remained substantially unchanged after the first cycle, which could underpin the durability and stability of surfactant-free Pd@pSiO<sub>2</sub> yolk-shell nanoparticles.

**Table 2.** Comparison of catalytic activity on oxidation of benzyl alcohol with previously reported nanocatalysts

Catalyst	Oxidant	Time (h)	Conv. (%)	Reference
Fe <sub>3</sub> O <sub>4</sub> @MIL-101	TBHP	12	2	34
Fe <sup>3+</sup> /TiO <sub>2</sub>	O <sub>2</sub>	1	77 <sup>a</sup>	36
Au/TiO <sub>2</sub>	O <sub>2</sub>	6	58	37
Au/NiAl-LDH	O <sub>2</sub>	0.5	53	38
Cu <sub>2</sub> O/Au	O <sub>2</sub>	5	90 <sup>a</sup>	39
Mn <sub>2</sub> O <sub>3</sub> nanorod	EDC	4	100	40

<sup>a</sup> Yield.

**Table 3.** Oxidation reaction of various substituted benzyl alcohols using surfactant-free Pd@pSiO<sub>2</sub> catalyst<sup>a</sup>

Entry	Substrate	Product	Conv. (%) <sup>b</sup>
1			>99
2			97
3			98
4			92
5			55
6			82
7			76
8			79
9			79
10			94

<sup>a</sup> Reaction condition: alcohols (1 mmol), Pd@pSiO<sub>2</sub> (0.1 mol% with respect to benzyl alcohol concentration), NaIO<sub>4</sub> as oxidant (5 equiv. to the substrate) at 150 °C for 18 h.

<sup>b</sup> Determined by <sup>1</sup>H-NMR. Conversions are based on the amount of applied alcohols used.

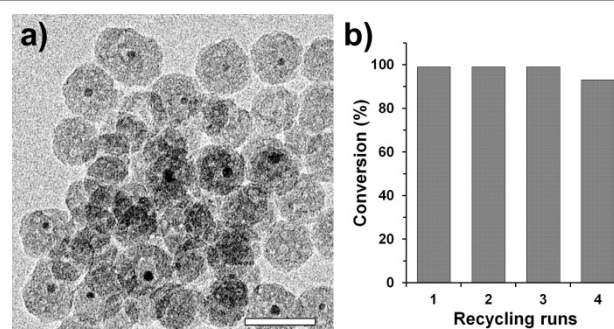


**Fig. 3** (a) TEM image of the surfactant-free Pd@pSiO<sub>2</sub> yolk-shell nanoparticles after the first cycle. The bar represents 40 nm. (b) Reuse of surfactant-free Pd@pSiO<sub>2</sub> yolk-shell nanoparticles

## Conclusions

In conclusion, a hybrid surfactant-free Pd@pSiO<sub>2</sub> yolk-shell nanostructure was developed, which helped achieve improved catalyst activity and thermal stability during reactions

employing this catalyst. The synthesis process was conducted in three steps, synthesis of: (1) Pd nanoparticles, (2) Pd@SiO<sub>2</sub> core-shell nanoparticles, and (3) Pd@pSiO<sub>2</sub> yolk-shell nanoparticles. The spherical Pd nanoparticles with a diameter of 3.4±0.2 nm were successfully coated with uniform layers of silica using a well-known water-in-oil microemulsion method. After hydrothermal etching and thermal treatment, the Pd@SiO<sub>2</sub> core-shell nanoparticles were transformed into corresponding Pd@pSiO<sub>2</sub> yolk-shell nanoparticles with randomly generated large pores inside the silica shell. This Pd@pSiO<sub>2</sub> yolk-shell nanoparticle exhibited excellent catalytic activity in the oxidation reaction of benzyl alcohol as well as that of various substituted benzyl alcohols.

The high catalytic activity, stability, and durability of the well-structured yolk-shell nanostructure developed in this study shows that this nanostructure can be used as a catalyst for a wide range of organic transformations.

### Acknowledgment

This research was supported by Basic Science Research Program through the National Research Foundation of Korea (NRF) funded by the Ministry of Science, ICT & Future Planning (No. 2012-005624) and the Human Resource Training Project for Regional Innovation (No. 2012H1B8A2026225). K.H.P thanks to the TJ Park Junior Faculty Fellowship and LG Yonam Foundation.

### Notes and references

1. S. H. Joo, J. Y. Park, C.-K. Tsung, Y. Yamada, P. Yang and G. A. Somorjai, *Nat Mater*, 2009, **8**, 126-131.
2. A. Schätz, O. Reiser and W. J. Stark, *Chemistry – A European Journal*, 2010, **16**, 8950-8967.
3. S. Shylesh, V. Schünemann and W. R. Thiel, *Angewandte Chemie International Edition*, 2010, **49**, 3428-3459.
4. L. Chen, J. Hu, Z. Qi, Y. Fang and R. Richards, *Industrial & Engineering Chemistry Research*, 2011, **50**, 13642-13649.
5. V. Polshettiwar, R. Luque, A. Fihri, H. Zhu, M. Bouhrara and J.-M. Basset, *Chemical Reviews*, 2011, **111**, 3036-3075.
6. S. Guo, S. Dong and E. Wang, *Small*, 2009, **5**, 1869-1876.
7. H. Ataee-Esfahani, L. Wang and Y. Yamauchi, *Chemical Communications*, 2010, **46**, 3684-3686.
8. R. Costi, A. E. Saunders and U. Banin, *Angewandte Chemie International Edition*, 2010, **49**, 4878-4897.
9. S. Guo, S. Dong and E. Wang, *ACS Nano*, 2010, **4**, 547-555.
10. Z. Liu, B. Zhao, C. Guo, Y. Sun, Y. Shi, H. Yang and Z. Li, *Journal of Colloid and Interface Science*, 2010, **351**, 233-238.
11. H. Zhang, Y. Yin, Y. Hu, C. Li, P. Wu, S. Wei and C. Cai, *The Journal of Physical Chemistry C*, 2010, **114**, 11861-11867.
12. C. An, R. Wang, S. Wang and X. Zhang, *Journal of Materials Chemistry*, 2011, **21**, 11532-11536.
13. J. Spadavecchia, C. Méthivier, J. Landoulsi and C.-M. Pradier, *ChemPhysChem*, 2013, **14**, 2462-2469.
14. C. Tan, X. Huang and H. Zhang, *Materials Today*, 2013, **16**, 29-36.
15. Y. Choi, H. S. Bae, E. Seo, S. Jang, K. H. Park and B.-S. Kim, *Journal of Materials Chemistry*, 2011, **21**, 15431-15436.
16. F.-h. Lin and R.-a. Doong, *The Journal of Physical Chemistry C*, 2011, **115**, 6591-6598.
17. S. W. Kang, Y. W. Lee, Y. Park, B.-S. Choi, J. W. Hong, K.-H. Park and S. W. Han, *ACS Nano*, 2013, **7**, 7945-7955.
18. G. M. Scheuermann, L. Rumi, P. Steurer, W. Bannwarth and R. Mülhaupt, *Journal of the American Chemical Society*, 2009, **131**, 8262-8270.
19. R. Li, P. Zhang, Y. Huang, P. Zhang, H. Zhong and Q. Chen, *Journal of Materials Chemistry*, 2012, **22**, 22750-22755.
20. M. Kim and H. Song, *Journal of Materials Chemistry C*, 2014, **2**, 4997-5004.
21. J. C. Park, E. Heo, A. Kim, M. Kim, K. H. Park and H. Song, *The Journal of Physical*

- Chemistry C*, 2011, **115**, 15772-15777.
22. M. Kim, E. Heo, A. Kim, J. Park, H. Song and K. Park, *Catal Lett*, 2012, **142**, 588-593.
23. H. R. Choi, H. Woo, S. Jang, J. Y. Cheon, C. Kim, J. Park, K. H. Park and S. H. Joo, *ChemCatChem*, 2012, **4**, 1587-1594.
24. M. Kim, J. C. Park, A. Kim, K. H. Park and H. Song, *Langmuir*, 2012, **28**, 6441-6447.
25. H. Woo, K. Lee and K. H. Park, *ChemCatChem*, 2014, **6**, 1635-1640.
26. H. Woo, K. Lee, J. C. Park and K. H. Park, *New Journal of Chemistry*, 2014, **38**, 5626-5632.
27. K. Yamaguchi, K. Mori, T. Mizugaki, K. Ebitani and K. Kaneda, *Journal of the American Chemical Society*, 2000, **122**, 7144-7145.
28. K. Mori, T. Hara, T. Mizugaki, K. Ebitani and K. Kaneda, *Journal of the American Chemical Society*, 2004, **126**, 10657-10666.
29. S. Ganesamoorthy, K. Shanmugasundaram and R. Karvembu, *Catalysis Communications*, 2009, **10**, 1835-1838.
30. V. Polshettiwar and R. S. Varma, *Organic & Biomolecular Chemistry*, 2009, **7**, 37-40.
31. J. Pritchard, L. Kesavan, M. Piccinini, Q. He, R. Tiruvalam, N. Dimitratos, J. A. Lopez-Sanchez, A. F. Carley, J. K. Edwards, C. J. Kiely and G. J. Hutchings, *Langmuir*, 2010, **26**, 16568-16577.
32. P. Miedziak, M. Sankar, N. Dimitratos, J. A. Lopez-Sanchez, A. F. Carley, D. W. Knight, S. H. Taylor, C. J. Kiely and G. J. Hutchings, *Catalysis Today*, 2011, **164**, 315-319.
33. Y. Chen, H. Wang, C.-J. Liu, Z. Zeng, H. Zhang, C. Zhou, X. Jia and Y. Yang, *Journal of Catalysis*, 2012, **289**, 105-117.
34. M. Saikia, D. Bhuyan and L. Saikia, *New Journal of Chemistry*, 2015, **39**, 64-67.
35. R. L. Oliveira, D. Zanchet, P. K. Kiyohara and L. M. Rossi, *Chemistry-A European Journal*, 2011, **17**, 4626-4631.
36. S. Higashimoto, R. Shirai, Y. Osano, M. Azuma, H. Ohue, Y. Sakata and H. Kobayashi, *Journal of Catalysis*, 2014, **311**, 137-143.
37. A. Mehri, H. Kochkar, G. Berhault, D. F. C. Merchán and T. Blasco, *Materials Chemistry and Physics*, 2015, **149**, 59-68.
38. Y. Du, Q. Jin, J. Feng, N. Zhang, Y. He and D. Li, *Catalysis Science & Technology*, 2015.
39. K. S. Prasad, H.-B. Noh, S. S. Reddy, A. E. Reddy and Y.-B. Shim, *Applied Catalysis A: General*, 2014, **476**, 72-77.
40. H. Rahaman, R. M. Laha, D. K. Maiti and S. K. Ghosh, *RSC Advances*, 2015, **5**, 33923-33929.
41. K. Bendahou, L. Cherif, S. Siffert, H. L. Tidahy, H. Benaïssa and A. Aboukaïs, *Applied Catalysis A: General*, 2008, **351**, 82-87.
42. Y. Han, J. Jiang, S. S. Lee and J. Y. Ying, *Langmuir*, 2008, **24**, 5842-5848.